SIMULATION OF HIGH RESOLUTION SATELLITE IMAGERY
FROM MULTISPECTRAL AIRBORNE SCANNER IMAGERY FOR
ACCURACY ASSESSMENT OF FUSION ALGORITHMS

Boris Prinz, Rafael Wiemker, Hartwig Spitzer
II. Institut für Experimentalphysik
Universität Hamburg
Germany
Mail: B. Prinz / KOGS, Vogt-Kölln-Str. 30, 22527 Hamburg, FRG
WWW-Page: http://kogs-www.informatik.uni-hamburg.de/projects/Censis.html
E-mail: {prinz,wiemker}@informatik.uni-hamburg.de, hartwig.spitzer@desy.de

ABSTRACT

For the years 1997 to 2000 it is expected that a number of new satellites will be launched into orbit by private companies which are specified to deliver panchromatic imagery of the earth surface with a spatial resolution as fine as 1 m. In contrast to the panchromatic band, the spectrally resolved bands will have a four times coarser ground resolution. Therefore, image fusion algorithms will certainly be employed in order to produce 'sharpened' color imagery.

The new satellites have the potential of stimulating and expanding the remote sensing market for image products at a resolution around one meter. In order to prepare for this era we have examined image fusion algorithms using already available airborne imagery. This paper tests fusion algorithms on imagery which was simulated using multispectral images of an airborne scanner (DAEDALUS ATM) with an average resolution of 1 m.

The main advantage of a simulation of satellite images is the possibility to immediately check the deviation between the original 1 m imagery and the fused (1 m + 4 m) multispectral image. Thus, various fusion algorithms can be tested with regard to their accuracy concerning e. g. land cover classification or change detection.

The spectral accuracy of the fused imagery depends strongly on the spatial resolution and scene content. Therefore, accuracy assessments from e. g. SPOT + LANDSAT TM - fusion can certainly not simply be extrapolated down to 1 m imagery. We find that the spectral accuracy of the simulated fused imagery indeed varies with different fusion algorithms. Even though the spectral accuracy of the fused imagery turns out to be limited, we find consistent results of land cover classifications.

1 Announced Arrival of Commercially Available High Resolution Satellite Imagery – Applicability to Local Environmental Monitoring

For the years 1997 to 2000 it is expected that a number of new satellites will be launched into orbit by private companies (Gupta 1995, Doyle 1996) which are specified to deliver imagery of the earth surface of a spatial resolution as fine as 1 m.

This fine a resolution has so far been the privilege of airborne rather than spaceborne overhead imagery – at least as far as the civilian community and *multispectral* (in contrast to panchromatic) imagery is concerned. Airborne image flights have a longstanding importance for cadastre, local planning and environmental monitoring (e.g. the health status of public trees in the city of Hamburg is monitored on aerial Color Infrared (CIR) photographs). So far the necessary image flights are conducted by private enterprises on particular customer request. They are thus rather expensive.

Multispectral spaceborne imagery on the other hand has been exploited for a number of environmental issues (such as deforestation, desertification, plant stress, water polution, climate warming etc.) but always on a *global* or *regional* scale – due to its limited spatial resolution (LANDSAT TM images have a pixel size of 30 × 30 m).

With the arrival of meter-range spaceborne imagery which can be purchased off-the-shelf by local authorities at the moment when the demand arises, overhead imagery may become a serious option even for purposes of *local* interest which up to now could not justify the higher cost of image flights.

2 Simulation of High Resolution Satellite Imagery from Multispectral Airborne Scanner Imagery

Launch of the first of the announced satellites is expected as early as summer 1997. It can be assumed that the testing and calibration phase will last for the first year of operations. It has to be noted, however, that the schedule for all of the announced satellites already had to be delayed several times.

In the meantime, we are in the position to *simulate* the high resolution satellite imagery from airborne scanner images of comparable spatial resolution. The imagery was recorded by a DAEDALUS AADS 1268 line scanner with $N = 10$ spectral bands on board a Dornier Do 228 aircraft during five campaigns from 1991 to 1997 in cooperation with the German Aerospace Research Establishment (DLR) at flight altitudes of 300 m, 900 m and 1800 m. The 300 m imagery has a nadir-looking ground resolution of 70 cm. Due to the panorama characteristic of so-called 'whisk broom' - line scanners and the large swath angle of $\pm 43°$, the ground resolution degrades to 1.40 m towards the image margins. The resolution is usually also slightly degraded by the resampling process required by georeferencing (which is compulsory for a number of applications). On average, the images have a resolution of 1 m, equally for all 10 spectral bands.

For all environmental image analysis purposes it is essential to have a spectral band in the near infrared (NIR). There, vegetation has a very high reflectance and is the most distinct from non-vegetation land cover. Also, plant health and plant stress show up in the increase of reflectance between the red and the NIR. Therefore we have simulated a photographic CIR image, where the spectral bands of Green, Red and the (invisible) Near Infrared (G,R,NIR) are coded by Blue, Green

Figure 1: Panchromatic image of urban area near the airport of Nürnberg, resolution 1 m.

Figure 2: Simulated color infrared image of urban area, resolution 4 m.[1]

and Red (R,G,B), respectively, and merged into a composite pseudo-color image.

The specifications of the high resolution satellites indicate that the 1 m resolution will only be reached for the panchromatic imagery. The spectrally resolved bands will come in a spatial resolution of only 4 m. We have simulated both the panchromatic full resolution image (Figure 1, by weighted average of the spectral bands) and the spectral band images (Figure 2, by averaging each 4×4 pixel window into one new pixel).[1]

3 Data Fusion between 1 m Panchromatic and 4 m Color Imagery

For local environmental applications we need both the spectral resolution (i.e., at least three distinct spectral bands: G,R,NIR) and good spatial resolution. Therefore, a fusion between the well resolved panchromatic and the four times coarser multispectral images is necessary.

Numerous efforts have been made to fuse data received from the same scene but different sensors (Shen et al. 1994, Darvishsefat 1995, Zhukov et al. 1995, Patterson et al. 1996, Peytavin 1996, Zhukov et al. 1996). Particular respect has been paid to the merging of image data with differing spatial resolution. If the two sensors do not operate from the same platform, the geometric rectification and registration of the images is a prerequisite to data fusion. Experience has shown

this to be a relatively easy process for satellite imagery (stable orbits and altitudes, small swath angles), but a rather cumbersome procedure for airborne line scanner imagery (flight track and altitude variations). In the particular case of the expected high resolution satellites this is not an issue since both the panchromatic and the multispectral image data are recorded from the same platform.

3.1 Fusion by HSV Transformation

The most widely applied fusion procedure is the merging of panchromatic SPOT imagery (10 m) with three-color SPOT imagery (20 m) or multispectral LANDSAT TM imagery (30 m). The simplest, most wide-spread and probably most intuitive technique works as follows (Kraus 1990, Albertz 1991):

1. Take three spectral bands from the multispectral imagery;

2. register the low resolution color image to the high resolution panchromatic image (i.e. essentially to magnify the color image to the same pixel size as the panchromatic image);

3. transform the magnified color image from an RGB color system into the HSV color system (Hue, Saturation, Value; see Foley et al. (1995));

4. replace the "Value" image by the high resolution panchromatic image;

5. transform back into the RGB color system.

This technique is known to work well for moderate resolution ratios (such as 1:3 for SPOT + LANDSAT TM). The results

---

[1] Postscript and PDF versions of this paper containing color images can be downloaded from
http://kogs-www.informatik.uni-hamburg.de/projects/censis /publications.html.

Figure 3: Fusion by HSV transformation.

Figure 4: Color infrared image of urban area, after bilinear interpolation of 4 m-image.[1]
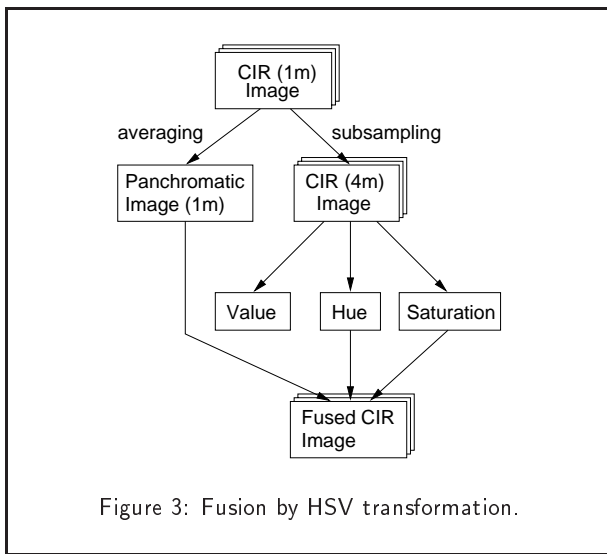
are still helpful but less reliable for resolution ratios such as 1:20, e.g. for fusion of SPOT color images with panchromatic aerial photography (Ersbøll et al. 1997).

In Figure 3 the steps involved in simulating the panchromatic and color infrared image and the fusion by HSV transformation are shown as a flow chart.

It has to be noted, however, that fusion by HSV transformation can be applied only to multispectral imagery consisting of three bands, since the image has to be coded as an RGB image before fusion can take place.

3.2 Fusion by Relative Contribution

Because the results of the fusion by HSV transformation were not fully satisfactory, also a second fusion method was examined, which can be described by the equation

$$F = \frac{MUL_{4m}}{PAN_{4m}} \cdot PAN_{1m} \qquad \text{(for each pixel)}$$

where F is the newly created fused image, MUL_{4m} is the multispectral (color infrared) image with 4 m resolution, PAN_{1m} is the highly resolved panchromatic image, and PAN_{4m} is a panchromatic image created by averaging the three bands of the multispectral image. In principle the first term in the above equation describes the spectral information while the spatial information is represented by the panchromatic image PAN_{1m}.

In contrast to the HSV transformation this fusion method produced images which were better correlated to those truly sampled at 1 m (see Section 4.1). Another advantage of this technique is that it is possible to fuse images with any number of bands, that cannot be coded by red, green and blue.

The result of an application of this technique to the examplary image shown here can be seen in Figure 5. In addition to the above recipe (Section 3.1), after the magnification of the color image (step 2), the color image was smoothed in a sliding local window of the size of the resolution ratio (here 4×4 pixels). This amounts to a bilinear interpolation between the known color values at the coarse resolution grid, and achieves the surprisingly 'sharp-looking' CIR image (Figure 4).
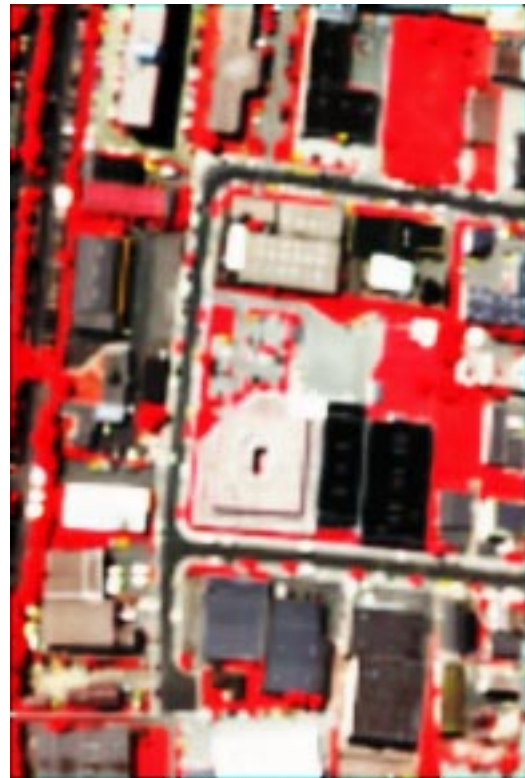
Figure 5: Color infrared image of urban area, fused from panchromatic image at (1 m) and color infrared image (4 m).[1]

4 Comparison between Fused Image and Full-Resolution Image

Although the result of the fusion looks very satisfactory to the eye, its spectral truth remains to be checked quantitatively.

When the real satellite imagery becomes available, data fusion in order to yield high resolved color images will certainly be performed. However, the accuracy of the estimated color values will remain unknown, and thus also the errors which propagate through later image processing steps such as land cover classification, change detection, NDVI computation, etc.

In contrast, with the airborne / simulated imagery we are in a position to immediately check the deviation between the multispectral imagery which is truly sampled with 1 m ground resolution and the one interpolated from 4 m resolution by data fusion with 1 m panchromatic resolution. The following quantitative comparisons can be made:

- We can directly regress the true intensity or reflectance values against the fusion-estimated values for each spectral band and determine the correlations.

- We can determine the root mean square deviation in reflectance between true and fusion-estimated values.

- The NDVI-values (normalized difference vegetation index, used for vegetation health monitoring) can be computed and compared to the full-resolution imagery.

- The true and the fusion-derived imagery can be classified into land cover classes (Richards 1993). Between the two results, a confusion matrix can be calculated and a statistical indicator of agreement ('Kappa coefficient', Congalton (1991)) on the overall classification accuracy of the fusion-estimated imagery in comparison to the true 1 m imagery.

In the following, the results of the above comparisons are described.

4.1 Correlation between Original and Fused Image

Since the color infrared image truly sampled at 1 m is available, the correlation between this original image and the fused image can be calculated directly. In Figure 6 the correlation between an original image with a resolution of 1 m and the fusion-derived image is shown for the bands Near Infrared, Red and Green. The fusion method applied here was the HSV transformation. Each pixel defined by its spatial coordinates has two reflectance values, one in the original and one in the fused image, so every point in the scatterplot represents one pixel. If both images were identical, all the points would be located on the straight line which is also plotted for orientation.

While the correlation between both images is very good in the red and green bands, the near infrared seems to be less correlated. The graphs in Figure 7 show the correlations of the same scene, but here the fused image was obtained by the relative contributions method.

The following table contains the correlation coefficients corresponding to the graphs in Figures 6 and 7:

Figure 6: Correlation between original image sampled at 1 m and image fused by HSV transformation.
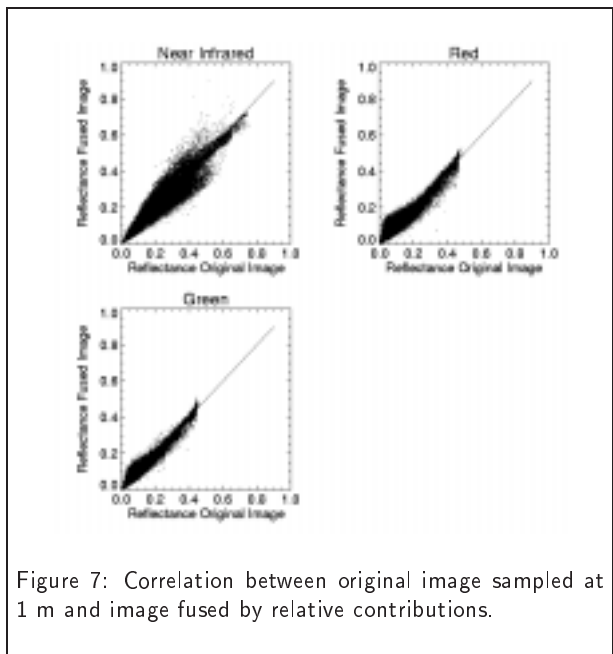
Figure 7: Correlation between original image sampled at 1 m and image fused by relative contributions.

Fusion method	Correlation coefficient		
	Near infrared	Red	Green
HSV transformation	0.82	0.96	0.97
Relative contributions	0.96	0.98	0.98
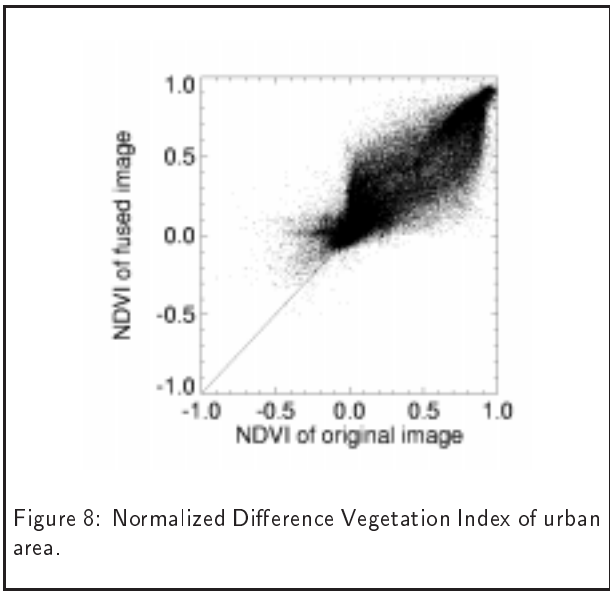
Figure 8: Normalized Difference Vegetation Index of urban area.
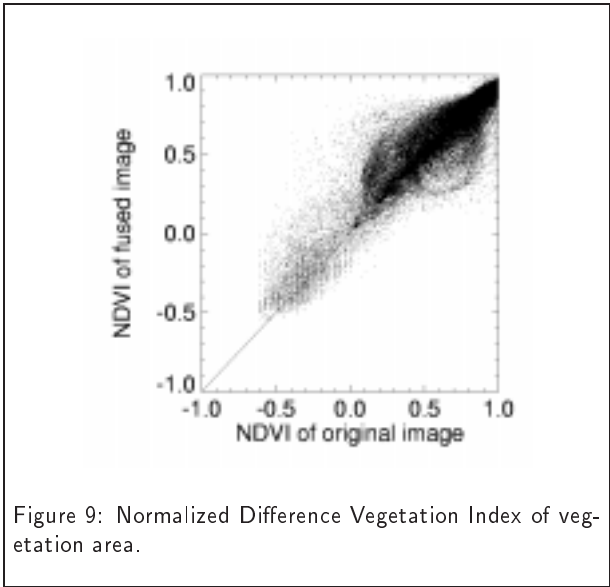
Figure 9: Normalized Difference Vegetation Index of vegetation area.

The reason for the rather low correlation coefficients caused by the HSV transformation is probably due to the way the "Value" image is produced. The HSV transformation as it is described by Foley et al. (1995) assigns the maximum brightness of the red, green and blue channel to the "Value". Therefore, the "Value" does not correspond directly to the panchromatic intensity which is an average of the three bands. In this regard it becomes questionable to replace the "Value" image with the panchromatic image.

4.2 Normalized Difference Vegetation Index

The normalized difference vegetation index (NDVI) which is used e. g. for vegetation health monitoring is defined by

$$\mathrm{NDVI} = \frac{\mathrm{NIR} - \mathrm{R}}{\mathrm{NIR} + \mathrm{R}} \in [-1, +1]$$

where NIR is the near infrared band and R is the red band. In Figure 8 the NDVI values of the original and the fused color infrared image are regressed for the exemplary image showing an urban area (Figure 1). The correlation coefficient for this image is $\rho = 0.87$ while the root mean square deviation is $\sigma = 0.16$.

Similarly, in Figure 9 the same variables are plotted for the vegetation area shown in Figure 10. Here, the correlation coefficient is higher ($\rho = 0.90$) and the deviation lower ($\sigma = 0.11$) than that of the urban area image. The reason for this is the lower spectral variability of the vegetation image. While in the urban area there are many transition lines from vegetation to non-vegetation, the vegetation image is quite uniform. Therefore, the blurring of the spectral information induced by fusion has a smaller effect on the latter image.

5 Classification

One of the most wide-spread applications for multispectral images is ground cover classification. For the assessment of classification agreement between true and fusion-derived imagery the Iterative Optimization Clustering (or Migrating Means) k-means algorithm as described e. g. by Richards (1993) was used. The initial clusters in the spectral domain were chosen randomly and the pixels were assigned iteratively

Figure 10: Vegetation area near Nürnberg.[1]

to the currently nearest candidate cluster on the basis of the Euclidean distance measure.

First, the original image truly sampled at 1 m was classified into a particular number of ground cover classes. The such found cluster centers were then used again to classify the fused images. This ensures that it is meaningful to compute a confusion matrix and a kappa coefficient (Congalton 1991) in order to quantify the error induced by fusion.

5.1 Classification Agreement

When two images are classified, the agreement of classification can be expressed by a confusion matrix (Richards 1993). As an example, the following confusion matrix was found after both the true and fused image of the urban area (Figure 1) were classified into three ground cover classes:

		Original Image Class			
		A	B	C	Σ
Fused	A	117481	0	2136	119617
Image	B	0	11274	2	11276
Class	C	2069	171	106867	109107
	Σ	119550	11445	109005	240000

The pixels that were assigned to the same class twice are on the diagonal, while the other matrix elements represent the numbers of pixels classified into different classes. In the above example there is no confusion between the classes A and B, virtually no confusion between B and C, and only a slight confusion between A and C.

To quantify the agreement of classification, the kappa coefficient (Congalton 1991) can be used, which is defined by

$$\kappa = \frac{p_0 - p_z}{1 - p_z},$$

where p_0 is the overall accuracy given by the sum over the diagonal matrix elements:

$$p_0 = \frac{1}{N} \sum_i X_{ii}.$$

From this number the fraction p_z of pixels that could have been accidentally classified correctly has to be subtracted:

$$p_z = \frac{1}{N^2} \sum_i \left(\sum_j X_{ij} \cdot \sum_j X_{ji} \right).$$

This has to be done, because even if the pixels were assigned to the classes completely at random, some pixels would nevertheless be assigned to the same class for both images.

The kappa coefficient for the above confusion matrix is $\kappa = 0.97$, which would be assessed as an excellent agreement (Ortiz et al. 1997).

Both the original and fused images of the two scenes (urban, vegetation) were classified, while varying the number of classes. The result is shown in Figure 11.

Generally, the kappa coefficient decreases with increasing number of classes, which can be explained by the increasing number of transition areas between classes in the image. At these land cover class borders, the multispectral information is blurred and misclassification occurs. Furthermore, the
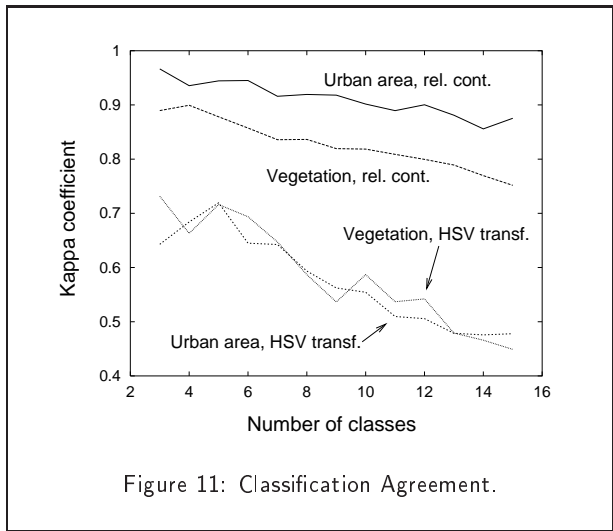
Figure 11: Classification Agreement.

fusion using relative contributions gives a better agreement of classification, which is due to the better correlation between the images, as shown in Section 4.1. Another effect that is observed is that the urban area image is classified more consistently, which is due to the greater variation in the spectral information. In the vegetation example, the classes are very similar, so that misclassification becomes more probable.

6 Summary

High resolution satellite imagery was simulated using airborne scanner imagery and two different fusion algorithms were applied to the data. The advantages of the fusion by relative contributions compared with HSV transformation are a better correlation between the original (1 m) and the fused (1 m + 4 m) imagery and the applicability to multispectral imagery with more than three bands. If the four times coarser multispectral image is smoothed before the fusion process, the resulting images do not only look better to the eye but also show a better correlation.

The comparison of fused and full resolution images showed that NDVI-computations and land cover classification strongly depend on the applied fusion method and scene content.

If fusion by relative contributions is used, the agreement of classification (kappa coefficient) between original and fused images is generally very high. The kappa coefficient decreases with an increasing number of classes, since more transitions between classes are introduced, where misclassification can occur due to the blurred spectral information. It emerged that the classification agreement also strongly depends on the variability of the scene content, i.e. the kappa coefficient is higher for images with a wider range of spectral classes.

REFERENCES

Albertz, J. (1991). *Grundlagen der Interpretation von Luft- und Satellitenbildern.* Wissenschaftliche Buchgesellschaft, Darmstadt, 1991.

Congalton, R. (1991). A Review of Assessing the Accuracy of Classifications of Remotely Sensed Data. *Remote Sensing of Environment* **37**, 35–46, 1991.

Darvishsefat, A. A. (1995). Einsatz und Fusion von Multisensoralen Satellitendaten zur Erfassung von Waldinventuren. Technical report, University of Zurich, Department of Geography, Remote Sensing Series, vol. 24, 1995.

Doyle, F. J. (1996). Thirty Years of Mapping from Space. In *Proceedings of the XVIII. Congress of the International Society for Photogrammetry and Remote Sensing ISPRS 1996, Vienna*, volume XXXI part B4 of *International Archives of Photogrammetry and Remote Sensing*, pages 227–230, 1996.

Ersbøll, B.K., T.H. Nielsen, and K. Conradsen (1997). On Fusion of High (Spatial) Resolution Greyscale Imagery with Low (Spatial) Resolution Color Imagery. In *Proceedings of the Third International Airborne Remote Sensing Conference and Exhibition, Copenhagen*, Ann Arbor, 1997, volume II, page 337 (1 page). Environmental Research Institut of Michigan.

Foley, J., A. Van Dam, S. Feiner, and J. Hughes (1995). *Computer Graphics: Principles and Practice.* Addison-Wesley, Reading, MA, 1995.

Gupta, Vipin (1995). New Satellite Images for Sale. *International Security* **20** (1), 94–125, 1995.

Kraus, K. (1990). *Fernerkundung, Band 2 – Auswertung photographischer und digitaler Bilder.* Dümmler, Bonn, 1990.

Ortiz, M. J., A. R. Formaggio, and J. C. N. Epiphanio (1997). Classification of Croplands through Integration of Remote Sensing, GIS and Historical Database. *International Journal of Remote Sensing* **18** (1), 95–105, 1997.

Patterson, T.J., R. Haxton, M.E. Bullock, and S.B. Ulinski (1996). Quantitative Comparison of Multispectral Image-Sharpening Algorithms. In *Proc. SPIE – Int. Soc. Opt. Eng. (USA), Orlando*, volume 2758, pages 168–179, 1996.

Peytavin, L. (1996). Cross-Sensor Resolution Enhancement of Hyperspectral Images Using Wavelet Decomposition. In *Proc. SPIE – Int. Soc. Opt. Eng. (USA), Orlando*, volume 2758, pages 193–203, 1996.

Richards, J. A. (1993). *Remote Sensing Digital Image Analysis.* Springer, Heidelberg, New York, 1993.

Shen, S.S., J.E. Lindgren, and P.M. Payton (1994). Panchromatic Band Sharpening of Multispectral Image Data to Improve Machine Exploitation Accuracy. In *Proc. SPIE – Int. Soc. Opt. Eng. (USA), San Diego*, volume 2304, pages 124–131, 1994.

Zhukov, B., M. Berger, F. Lanzl, and H. Kaufmann (1995). A New Technique for Merging Multispectral and Panchromatic Images Revealing Sub-Pixel Spectral Variation. In Stein, T.I., editor, *Proceedings of the International Geoscience and Remote Sensing Symposium, Florence, IGARSS 1995*, volume 3, pages 2154–2156. IEEE Catalog 95CH35770, 1995.

Zhukov, B., D. Oertel, P. Strobl, F. Lehmann, and M. Lehner (1996). Fusion of Airborne Hyperspectral and Multispectral Images. In *Proc. SPIE – Int. Soc. Opt. Eng. (USA), Orlando*, volume 2758, pages 148–159, 1996.